

AWARD NUMBER: W81XWH-22-1-0933

TITLE: Photovoltaic Substitute for Lost Photoreceptors in Retinal Injury or Degeneration

PRINCIPAL INVESTIGATOR: Prof. Daniel Palanker

CONTRACTING ORGANIZATION: Stanford University, Stanford, CA

REPORT DATE: October 2023

TYPE OF REPORT: Annual

PREPARED FOR: U.S. Army Medical Research and Development Command  
Fort Detrick, Maryland 21702-5012

DISTRIBUTION STATEMENT: Approved for Public Release;  
Distribution Unlimited

The views, opinions and/or findings contained in this report are those of the author(s) and should not be construed as an official Department of the Army position, policy or decision unless so designated by other documentation.

# REPORT DOCUMENTATION PAGE

*Form Approved*  
OMB No. 0704-0188

Public reporting burden for this collection of information is estimated to average 1 hour per response, including the time for reviewing instructions, searching existing data sources, gathering and maintaining the data needed, and completing and reviewing this collection of information. Send comments regarding this burden estimate or any other aspect of this collection of information, including suggestions for reducing this burden to Department of Defense, Washington Headquarters Services, Directorate for Information Operations and Reports (0704-0188), 1215 Jefferson Davis Highway, Suite 1204, Arlington, VA 22202-4302. Respondents should be aware that notwithstanding any other provision of law, no person shall be subject to any penalty for failing to comply with a collection of information if it does not display a currently valid OMB control number. **PLEASE DO NOT RETURN YOUR FORM TO THE ABOVE ADDRESS.**

<b>1. REPORT DATE</b> October 2023		<b>2. REPORT TYPE</b> Annual		<b>3. DATES COVERED</b> 01Sep2022-31Aug2023	
<b>4. TITLE AND SUBTITLE</b>  Photovoltaic Substitute for Lost Photoreceptors in Retinal Injury or Degeneration				<b>5a. CONTRACT NUMBER</b> W81XWH-22-1-0933	
				<b>5b. GRANT NUMBER</b>	
				<b>5c. PROGRAM ELEMENT NUMBER</b>	
<b>6. AUTHOR(S)</b>  Prof. Daniel V. Palanker  E-Mail: palanker@stanford.edu				<b>5d. PROJECT NUMBER</b>	
				<b>5e. TASK NUMBER</b>	
				<b>5f. WORK UNIT NUMBER</b>	
<b>7. PERFORMING ORGANIZATION NAME(S) AND ADDRESS(ES)</b>  Stanford University, 452 Lomita Mall, Room 135, Stanford, CA 94305-4085				<b>8. PERFORMING ORGANIZATION REPORT NUMBER</b>	
<b>9. SPONSORING / MONITORING AGENCY NAME(S) AND ADDRESS(ES)</b>  U.S. Army Medical Research and Development Command Fort Detrick, Maryland 21702-5012				<b>10. SPONSOR/MONITOR'S ACRONYM(S)</b>	
<b>12. DISTRIBUTION / AVAILABILITY STATEMENT</b>  Approved for Public Release; Distribution Unlimited				<b>11. SPONSOR/MONITOR'S REPORT NUMBER(S)</b>	
<b>13. SUPPLEMENTARY NOTES</b>					
<b>14. ABSTRACT</b>  Ocular trauma or laser injury, as well as retinal degeneration, can lead to loss of photoreceptors, resulting in a permanent visual impairment. Our photovoltaic substitute of the photoreceptors directly converts light into pulsed electric current in each pixel, stimulating the second-order retinal neurons. Recent clinical tests in patients blinded by retinal degeneration demonstrated safety of this approach and prosthetic visual acuity closely matching the 100µm pixel pitch of the implant. To further improve visual acuity, we are developing smaller pixels, down to 20µm, based on three-dimensional honeycomb design. In particular, we study integration of such implants with the retina, the optimal geometry of the honeycomb electrodes for the highest spatial resolution and selectivity of the retinal activation, as well as a long-term follow-up of the retinal excitability with such implants.  Upon successful completion of the proposed development and preclinical testing, this implant will be transferred to our industrial partner for clinical studies. This technology will benefit patients with traumatic retinopathy, laser injury and degenerative retinal diseases. Implants with adequately small pixels should support visual acuity sufficient for reading and face recognition, thereby enabling independent and productive lifestyle to the Service Members, veterans, and their family members.					
<b>15. SUBJECT TERMS</b> None listed.					
<b>16. SECURITY CLASSIFICATION OF:</b>			<b>17. LIMITATION OF ABSTRACT</b>  Unclassified	<b>18. NUMBER OF PAGES</b>  15	<b>19a. NAME OF RESPONSIBLE PERSON</b> USAMRDC
<b>a. REPORT</b>  Unclassified	<b>b. ABSTRACT</b>  Unclassified	<b>c. THIS PAGE</b>  Unclassified			<b>19b. TELEPHONE NUMBER</b> (include area code)

## TABLE OF CONTENTS

	<u>Page</u>
<b>1. Introduction</b>	<b>1</b>
<b>2. Keywords</b>	<b>1</b>
<b>3. Accomplishments</b>	<b>1</b>
<b>4. Impact</b>	<b>7</b>
<b>5. Products</b>	<b>7</b>
<b>6. Participants &amp; Other Collaborating Organizations</b>	<b>8</b>
<b>7. Changes/Problems</b>	<b>10</b>
<b>8. Special Reporting Requirements</b>	<b>10</b>
<b>9. Appendices</b>	<b>12</b>

## 1. Introduction:

Shear forces, laser injury or disease may lead to blindness due to loss of photoreceptors. We developed a photovoltaic substitute for the photoreceptors, which directly converts light into pulsed electric current in each pixel, stimulating the nearby inner retinal neurons. Feasibility trial in human patients with 100 $\mu$ m pixels confirmed the safety, stability of such implants and spatial resolution matching the pixel size (on average 1.17 pixels corresponding to 20/500 Snellen acuity). We are working now on implants with smaller pixels for highly functional restoration of sight. To enable sufficiently deep penetration of electric field into the retina with smaller pixels, we developed 3-dimensional honeycomb arrays with pixels of 20, 30 and 40 $\mu$ m in width, and now study the anatomy of retinal migration into the implants in-vivo. To assess functional performance of such implants we will first manufacture photovoltaic arrays with prototype honeycombs using 3-D polymerization and test their functional integration with the retina. After selecting the optimal pixel dimensions, we will manufacture the conductive honeycombs for local return electrodes, integrate them with photovoltaic arrays and measure stimulation thresholds, spatial resolution, and dynamic range of prosthetic vision.

**2. Keywords:** Retinal injury, retinal degeneration, retinal prosthesis, photovoltaic

## 3. Accomplishments:

### The major goals of the project

Tasks	Time, months	% complete
<b>Specific Aim 1</b> <b>Study the cellular composition of the retinal tissue migrating into the honeycomb implants with pixels of 20, 30, 40 <math>\mu</math>m in width</b>		
Subtask 1 Submit documents to ACURO.	1-3	100
Milestone: ACURO approval obtained.		
Subtask 2 a) Fabricate Si implants composed of 4 quadrants: honeycomb-shaped pixels of 20, 30, 40 $\mu$ m in width and a flat control. b) Passivate the arrays by thermal oxidation and metallization using gold and titanium.	1-6 1-12	100% 100%
Milestone(s): Fabricated the passivated Si arrays with honeycomb cavities of 40, 30 and 20 $\mu$ m in size and a flat control.		
Subtask 3 a) Implant these arrays into RCS rats for 6 weeks. b) Using cell type-specific fluorescent antibodies, quantify the distribution of the neural and glial cells	6-24 6-24	75% 50%

<p>in the retina inside and around the honeycombs of various sizes and with various coatings.</p> <p>c) If metal coatings cause cellular irritation, add the insulating coating on top.</p>	12-24	25%
<p>Milestone(s): Established the optimal biocompatible coating of the implants and the minimum size of the cavities for efficient retinal integration with the 3-D implant.</p>		
<p><b>Specific Aim 2</b>  <b>Fabricate the monopolar photovoltaic arrays with vertical PN junction and pixel sizes of 20, 30, 40 and 55µm. Build the polymer honeycombs on such flat implants and test the retinal excitability over time.</b></p>		
<p>Subtask 1</p> <p>a) Fabricate the flat monopolar photovoltaic arrays with vertical PN junction and pixels of 20, 30, 40 and 55 µm in size.</p> <p>b) Optimize the SIROF electrode thickness and activation protocol for the maximum charge injection in electrolyte.</p> <p>c) Characterize the electrode-electrolyte interface with various electrode sizes using electrochemical impedance spectroscopy.</p>	1-12	75%
	6-18	25%
	6-18	25%
<p>Milestone(s): Built the flat photovoltaic monopolar arrays, characterized and optimized the SIROF electrodes</p>		
<p>Subtask 2</p> <p>a) Add the photoresist-based honeycomb walls to these flat arrays using multiphoton polymerization tool.</p> <p>b) Using the electrochemical impedance spectroscopy, characterize the impedance of these 3-D structures in electrolyte.</p> <p>c) Using a scanning pipette electrode, characterize the current dynamics over the array in electrolyte under pulsed lighting at various frequencies.</p>	12-18	50%
	12-24	
	12-24	25%

Milestone(s): Built the active implants with 3-D polymer wells and characterized the electric field dynamics in electrolyte.		
Subtask 3		
a) Implant the photovoltaic arrays with and without the polymer honeycombs and the skull electrodes.	18-24	25%
b) Using VEP recordings, measure the full-field stimulation threshold and dynamic range with honeycomb implants and flat controls over 6 months follow-up.	18-30	25%
c) Using synaptic blockers, check the selectivity of the bipolar cells' stimulation with 3-D monopolar implants and flat bipolar controls.	18-30	
Milestone(s): Changes in the retinal excitability over time with 3-D implants are assessed. Selectivity of the bipolar cells' stimulation with monopolar and bipolar implants is established.		
<b>Specific Aim 3</b> <b>Develop the conductive honeycombs for local return electrodes and shunt resistor, integrate them with the photovoltaic arrays and measure the stimulation thresholds, selectivity and spatial resolution of prosthetic vision.</b>		
Subtask 1		
a) Electroplate the honeycomb walls. Check their structural integrity and capacitance in electrolyte.	12-24	10%
b) Deposit SIROF on top of the walls as a local return electrode. Assess the electrode capacitance in electrolyte using electrical impedance spectroscopy (EIS).	18-24	
Milestone: Electroplating of the conductive honeycombs is developed, they are characterized and integrated with the photovoltaic pixels.		
Subtask 2	1-24	
	18-24	25%

<p>a) Develop a shunt resistor for discharging the electrodes between the pulses, optimized for each pixel size.</p> <p>b) Integrate the shunt resistor into the pixels under the electrodes.</p>		
<p>Milestone: Shunt resistors are developed and integrated into the photovoltaic pixels of the implants.</p>		
<p>Subtask 3</p> <p>a) Implant the photovoltaic arrays with conductive honeycombs of various pixel sizes in RCS rats.</p> <p>b) Using VEP recordings and synaptic blockers, measure the selectivity of the network-mediated retinal stimulation.</p> <p>c) Measure the full-field stimulation threshold and dynamic range of the response over 6 months follow-up.</p> <p>d) Measure the spatial resolution based on the cortical response to alternating gratings.</p>	<p>24-36</p> <p>24-30</p> <p>30-36</p> <p>30-36</p>	
<p>Milestone(s): Established the selectivity of the network-mediated retinal stimulation, spatial resolution of prosthetic vision and stimulation threshold over the 6 months follow-up period.</p>		

## What was accomplished under these goals?

### Migration of the inner retinal neurons into the implants

To assess the migration of the target bipolar cells and other inner retinal cells into honeycomb wells, 1 mm wide and 30µm thick silicon devices (Fig. 1c-d) were implanted into the subretinal space of RCS rats (6 to 9 months old, n = 33) for 6 weeks. Each device comprised of four quadrants (Fig. 1c): flat, 20, 30 and 40 µm honeycombs to assess the effect of pixel size on retinal integration. The 25 µm height of the walls was chosen to accommodate the migration of second-order neurons (primarily BCs) and exclude the third-order neurons (ACs and RGCs) from the wells.

Characterization of cellular integration with the implants was performed on reconstructed confocal acquisitions of the whole-mounted retina-honeycomb-sclera complex. Overview of the implant from the top of the honeycomb to the base of the well reveals a uniform fill by rod and cone bipolar immuno-labeled cells along with other non-labeled DAPI nuclei throughout the wells of different sizes (Fig. 2a, c, e). Cross-sectional (side) views through a randomly selected honeycomb row, projected from the middle of the wells to the sidewall, show migration to the base of the implants, while some BCs remain above the honeycomb walls. The fraction of the rod BCs, relative to its average number in the non-implanted control, inside the 25 µm walls of 20, 30 and 40 µm honeycombs was  $0.64 \pm 0.31$ ,  $0.77 \pm 0.31$ ,  $0.53 \pm 0.14$ , respectively (Fig. 2i). For cone BCs these fractions were  $0.64 \pm 0.19$ ,  $0.75 \pm 0.15$ ,  $0.70 \pm 0.17$  respectively (Fig. 2j). Both bipolar cell types maintain their structural integrity, with unchanged stratification in the IPL.

The other type of second-order neurons, horizontal cells, undergo dendritic and axonal degeneration, but remain in similar numbers after photoreceptor degeneration in RCS retina, compared to healthy retina. Horizontal cells and their axons were observed close to the subretinal space in the non-implanted control and interfacing with the flat implant control. In the presence of the 3-D implants, most horizontal cells migrated into the honeycombs:  $0.85 \pm 0.09$ ,  $0.70 \pm 0.22$  and  $0.87 \pm 0.17$  in 20, 30 and 40 µm wells, respectively.

The third-order neurons of the INL, amacrine cells, play a major role in signal transduction and modulation between bipolar and ganglion cells. Therefore, direct electrical stimulation of the amacrine cells could lead to alteration of the natural signal processing. None of the immunolabeled subset of cholinergic starburst amacrine cells were observed inside the wells in the top-down view. Amacrine cell somas remain above the walls of all honeycomb sizes away from the electric field, and preserve a similar IPL stratification as in the non-implanted control.

### Inner retinal vasculature

An important consideration when dealing with retinal prosthesis is whether the device will allow normal oxygenation of migrated cells. Subretinal implants create a barrier between the choroidal supply and the retina. However, since the implants are inserted after a complete degeneration of photoreceptors, the choroidal supply is not necessary as the inner retina has its own vasculature. The inner retinal vasculature is grouped into the superficial vascular complexes (SVC; NFL to IPL) and the deep vascular complexes (DVC; IPL to OPL). The deep capillary plexus (DCP) of DVC comprises of vessels in the INL and OPL (subretinal space in degenerated RCS retina).

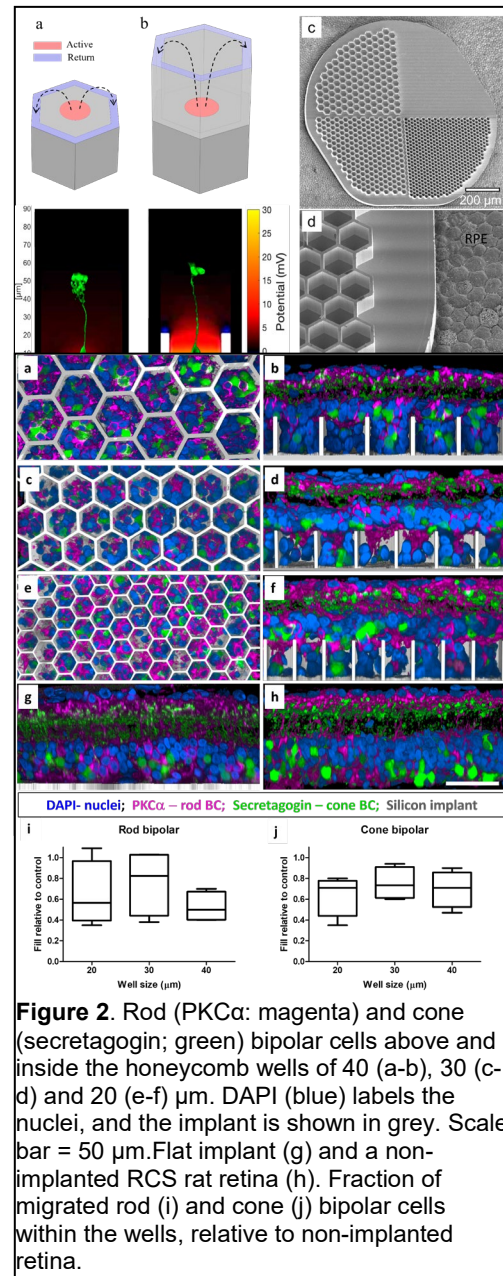


**Figure 2.** Rod (PKCα: magenta) and cone (secretagogin; green) bipolar cells above and inside the honeycomb wells of 40 (a-b), 30 (c-d) and 20 (e-f) µm. DAPI (blue) labels the nuclei, and the implant is shown in grey. Scale bar = 50 µm. Flat implant (g) and a non-implanted RCS rat retina (h). Fraction of migrated rod (i) and cone (j) bipolar cells within the wells, relative to non-implanted retina.

The presence of a flat subretinal implant does not affect the DCP density or location, as compared to non-implanted area. With a 3-dimensional device, the DCP vessels rest on top of the walls and do not migrate into the wells of any size studied. Nuclei (likely second-order neurons) migrate past the vessels into the wells and retain a healthy appearance 6-9 weeks after implantation, suggesting proper oxygenation and nutrients supply.

### Retinal glial response

Müller glia span the entire thickness of the retina and ensheath all its neurons. Müller cells were immunolabelled by its cytoplasmic enzyme glutamine synthetase (GS), and Müller cell nuclei - by its transcription factor, SOX9. Migration of the Müller cell nuclei is known to happen after the retinal damage [25], similar to subretinal surgery for implantation of flat and 3-D arrays. In the non-implanted control, Müller cell nuclei are arranged orderly in the middle of the INL. After retinal integration with the honeycombs, some of the Müller cell processes and nuclei can be observed inside the wells in the top-down view. Most of the Müller nuclei migrate into the 30  $\mu\text{m}$  and 40  $\mu\text{m}$  wells:  $0.73 \pm 0.06$  and  $0.70 \pm 0.08$ , respectively, but only  $0.36 \pm 0.12$  into 20  $\mu\text{m}$  wells relative to the non-implanted control. The side views show some Müller cell bodies even reaching the bottom of the larger wells, but very shallow penetration into the 20  $\mu\text{m}$  wells.

Another consequence of a retinal insult is the Müller cell activation, which may lead to glial scar formation. On a flat implant, glial scars may increase the distance and impedance between the active electrodes and the bipolar cells. This may be even more problematic with honeycomb implants as scar tissue could prevent migration of the bipolar cells into the wells and result in poor retinal stimulation. Müller cell activation was assessed by immunostaining the tissues with Glial Fibrillary Acidic Protein (GFAP), which is upregulated in Müller cells and astrocytes. GFAP activation and clusters (indicative of a glial scar; yellow arrows) can be observed in the INL of the non-implanted RCS retina and flat implant control. Migration of the Müller cells into the wells increased with the size of the honeycombs:  $0.43 \pm 0.07$ ,  $0.60 \pm 0.03$ ,  $0.71 \pm 0.12$  into 20  $\mu\text{m}$ , 30  $\mu\text{m}$  and 40  $\mu\text{m}$  wells, relative to the position of GFAP staining in the INL in non-implanted controls. In contrast, the average penetration depth of all nuclei does not exhibit the well-width selectivity:  $0.97 \pm 0.08$ ,  $1.00 \pm 0.11$ ,  $1.02 \pm 0.06$  of all INL nuclei, relative to the non-implanted control, migrate into 20  $\mu\text{m}$ , 30  $\mu\text{m}$  and 40  $\mu\text{m}$  pixels, respectively. Migration of neurons (Fig. 2) deeper than Müller cells into the wells (specially in 20  $\mu\text{m}$  wells) indicates that even the glial scar formation does not prevent movement of the retinal neurons into honeycombs.

### Retinal stimulation post migration

To assess whether the electrical excitability of the retina was affected by migration into the honeycombs, polymer-based non-conducting vertical walls were formed on flat arrays with photovoltaic pixels, having a common return electrode only near the periphery of the array (monopolar configuration; Fig. 1e) [26]. Electric field in such wells is oriented vertically, similarly to that expected with an elevated return electrode on top of conductive walls. Such arrays were implanted into the subretinal space of RCS rats, temporal-dorsal to the optic nerve head (Fig. 3a). Surgical success was assessed using OCT

immediately after the surgery, and migration was assessed six weeks after implantation. After surgery, the retina was separated from the implant by a thin layer of debris and fluid (Fig. 3 b, d). Six weeks after implantation, the

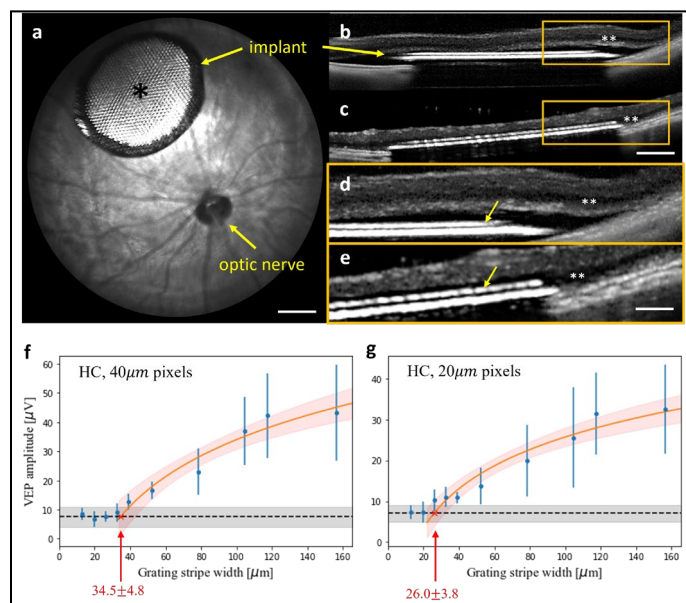


**Figure 3.** (a) Fundus of a rat eye with a subretinal honeycomb implant. Scale bar = 500  $\mu\text{m}$  (b) OCT image of the detached retina above the implant right after surgery and (c) 6 weeks later. Scale bar = 250  $\mu\text{m}$ . Migration of the INL (\*\*) into the honeycomb wells (yellow arrows) can be observed by comparing the higher magnification OCT at day 0 (d) and week 6 (e). Scale bar = 100  $\mu\text{m}$ . (f-g) VEP amplitude as a function of the grating bar width with honeycomb devices of (f) 40  $\mu\text{m}$  and (g) 20  $\mu\text{m}$  pixels. The black dashed lines represent the mean noise level. Red line is a logarithmic fit, which defines acuity as a crossing point with the noise level, pointed by the arrow.

INL is barely detectable by OCT above the honeycombs (Fig. 3c, e), but visible outside the implant, indicating the INL migration into the wells.

Visually evoked potentials (VEPs) were recorded via transcranial electrodes above the visual cortices, with NIR stimuli at 2 Hz, pulse duration of 10 ms and peak irradiance ranging from 0.002 to 4.7 mW/mm<sup>2</sup> on the retina. The VEP was assessed with monopolar flat devices having 20 μm and 40 μm pixels and with 3-D printed walls on similar pixels for comparison. Stimulation thresholds with the 3D devices (0.064 ± 0.034 mW/mm<sup>2</sup>) closely matched that of full-field stimulation with the flat implants (0.057 ± 0.029 mW/mm<sup>2</sup>), where neighboring pixels combine to align the E-field vertically. This suggests that not only is the number of bipolar cells preserved post migration (Fig. 2), but so is the electrical excitability of the retina. It is important to note that simultaneous activation of all the pixels in a monopolar array results in summation of their electric fields, adding up to a field similar to that of a single large electrode, equal in size to the whole array. Within the thickness of inner retina (< 0.1 mm), this field is nearly vertical, similar to the vertical field inside 3-D cavities. However, when single flat pixels (or sparse patterns) are activated, their electric field is much more divergent and shallower, and hence inferior to nearly vertical field inside 3-D cavities.

To assess the spatial resolution of prosthetic vision with honeycomb implants, we measured grating acuity after the cell migration is complete (> 8 weeks). As shown in Figure 3f, the fitting line crosses the noise level at 34.5 ± 4.8 μm, matching the pixel pitch of 40 μm hexagonal array (40·cos 30° = 34.6). As shown in Figure 3g, with 20 μm arrays, the measured acuity limit was much larger than the 17 μm pixel pitch: 26.0 ± 3.8 μm. Taking into account that in a rat eye, 1 degree of the visual angle corresponds to 65 μm on the retina, grating with 26 μm stripe width corresponds to 1.2 cycle per degree (cpd), matching the limit of natural visual acuity in rats.

### **(c) Animal Use Regulatory Protocols**

#### **Protocol ( 1 of total): 1**

*Protocol [ACURO Assigned Number]: 34286*

*Title: "Photovoltaic Substitute for Lost Photoreceptors in Retinal Injury or Degeneration - DoD 2022"*

*Target required for statistical significance: depends on the sub-group.*

*Target approved for statistical significance: 150 animals per year.*

**Submitted to and Approved by: the IACUC at Stanford University**

#### **Status:**

Approved through 05/23/2025

### **What do you plan to do during the next reporting period to accomplish the goals and objectives?**

Next, we plan to work on Aim 3, Subtask 1 and 2:  
Develop conductive honeycomb walls for local return electrodes and shunt resistors.

- 4. Impact:** Describe distinctive contributions, major accomplishments, innovations, successes, or any change in practice or behavior that has come about as a result of the project relative to:

Nothing to report.

- 5. Products:** List any products resulting from the project during the reporting period. If there are no products to report for the current quarter, state "Nothing to report."

*Examples of products include:*

- *publications, conference papers, and presentations;*
- *website(s) or other Internet site(s);*
- *technologies or techniques;*

- *inventions, patent applications, and/or licenses; and*
  - *other products, such as data or databases, biospecimen collections, germplasm, audio or video products, software, models, educational aids or curricula, instruments or equipment, data and research material, clinical or educational interventions, or new business creation.*
- Our manuscript “Cellular migration into a subretinal honeycomb-shaped prosthesis for high-resolution prosthetic vision” by M.B. Bhuckory et.al. is accepted to Proceedings of National Academy of Sciences, September 2023.

We presented 3 posters on ARVO 2023 annual conference: New Orleans, April 23-27, 2023

- Explantation of subretinal prostheses with planar and 3-D configurations. M. Bhuckory, et.al.
- Optimal Photovoltaic Pixels for High-Resolution Subretinal Prosthesis. Z.C. Chen et.al.
- Role of stimulation selectivity in visual acuity with subretinal prostheses. B. Wang et.al.

## 6. Participants & Other Collaborating Organizations

**Organization Name: Stanford University**

**Performance Location of Organization:**

**Hansen Experimental Physics Laboratory,  
452 Lomita Mall, Astrophysics Building,  
Room S05 & S04, Stanford, CA 94305-4085**

### 1. Prof. Daniel Palanker

Name:	Daniel Palanker
Project Role:	PI
Nearest person month worked:	1.7 CM
Contribution to Project:	General supervision and guidance of the project, setting goals and priorities, assessing results, reporting the outcomes.

### 2. Mr. Mohajeet Bhuckory

Name:	Mohajeet Bhuckory
Project Role:	Sr. Research Associate
Nearest person month worked:	1.0 CM
Contribution to Project:	Subretinal implantations, transcranial electrodes, in-vivo imaging, immunohistochemical tissue analysis.

### 3. Mr. Ludwig Galambos

Name:	Ludwig Galambos
Project Role:	Research Associate/Engineer
Nearest person month worked:	7.9 CM
Contribution to Project:	Support of the implant fabrication at the Stanford Nanofabrication Facility, students training, equipment maintenance and troubleshooting.

### 4. Mr. Theodore Kamins

Name:	Theodore Kamins
Project Role:	Adjunct Professor
Nearest person month worked:	3.0 CM
Contribution to Project:	Design of the implant fabrication processes and procedures: ion doping, lithographic processes, metal coatings, 3-D segmentation, etc.

### 5. Mr. Nathan Jensen

Name:	Nathan Jensen
Project Role:	Graduate Student
Nearest person month worked:	4.0 CM
Contribution to Project:	Computational modelling of the electric field in tissue, modelling on neural response to electrical stimulation, ex-vivo characterization and testing of the implants.

### 6. Mr. Andrew Shin

Name:	Andrew Shin
Project Role:	Graduate Student
Nearest person month worked:	5.0 CM
Contribution to Project:	Implants fabrication at Stanford Nanofabrication Facility, masks design and implementation, assessment of the fabrication processes.

### 7. Mr. Davis Pham-Howard

Name:	Davis Pham-Howard
Project Role:	Lab Technician
Nearest person month worked:	2.5 CM

Contribution to Project:	Animal protocols and compliance, animal maintenance during surgery and electrophysiological measurements, animal recovery, lab maintenance.
--------------------------	---

## 7. Changes/Problems:

### a. Actual Problems or delays and actions to resolve them

Nothing to report.

### b. Anticipated Problems/Issues

*Provide a description of anticipated problems or issues that have a potential to impede performance or progress. Also provide course of actions planned to mitigate problems or to take should the problem materialize.*

Nothing to report.

## 8. Special Reporting Requirements:

**Quad Charts:** If applicable, the Quad Chart (available on <https://www.usamraa.army.mil>) should be updated and submitted with attachments.

Attached below.



PI: Palanker, Daniel

Org: Stanford University

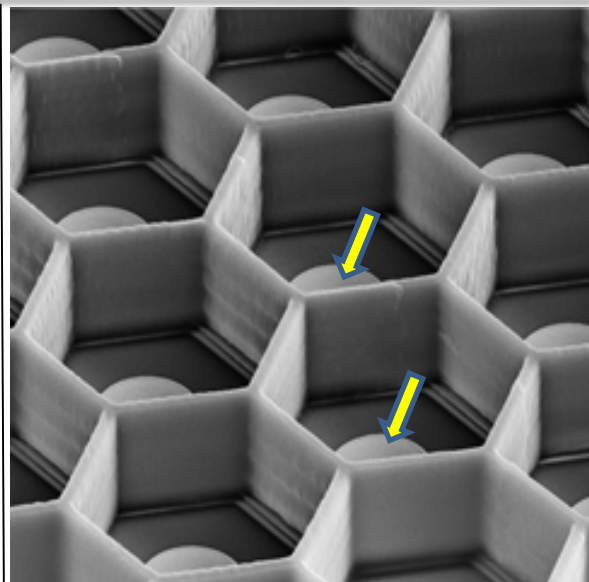
Award Amount: \$1,512,511 (9/1/2022-8/31/2025)

**Study/Product Aim(s)**

- Fabricate the passive honeycomb arrays with pixels of 20, 30 and 40µm and study retinal migration into the wells in-vivo.
- Make polymer prototypes of the honeycombs on active photovoltaic arrays and study retinal excitability after migration.
- Manufacture photovoltaic arrays with local return electrodes on honeycombs and measure the stimulation thresholds, spatial resolution and dynamic range of prosthetic vision using VEP measurements in-vivo.

**Progress summary**

We implanted passive 3-D arrays in subretinal space in RCS rats for 6-8 weeks, and then analyzed the tissue migration into the implants using immunohistochemical staining and confocal imaging of the whole-mount retinal explants. Using active implants with polymer honeycomb prototypes, we analyzed the full-field stimulation thresholds and visual acuity. With 25 µm high walls, the blood vessels and amacrine cells remain above the honeycomb walls while other INL cells migrate into the wells. Retinal migration into the honeycombs did not negatively affect its electrical excitability.



Active 40 µm pixels with polymer honeycomb walls. Yellow arrows indicate the electrodes. Photovoltaic pixels convert light into electric current to stimulate the secondary retinal neurons. Vertical walls around pixels direct electric current upward, thus reducing the stimulation threshold and enabling smaller pixels.

**Timeline and Cost**

Activities	CY	1	2	3
Study retinal migration into honeycombs				
Analyze retinal excitability with prototype honeycombs				
Assess visual acuity and dynamic range with honeycombs having local returns				
<b>Estimated Budget (\$K)</b>		\$544	\$494	\$475

**Goals/Milestones**

**CY1 Milestones:**

- Determine the limits of pixel size for retinal migration
- Establish the optimal height of the honeycomb walls for retinal integration.

**CY2 Milestones:**

- Assess retinal excitability changes upon migration into 3-D implants with a follow-up of one year

**CY3 Milestones:**

- Manufacture the honeycombs with local return electrodes.
- Measure simulation thresholds, spatial resolution and contrast sensitivity of prosthetic vision in rats with honeycomb arrays.

**Budget Expenditure to Date**

Projected Expenditure: \$494.3K (9/1/2023-8/31/2024)

Actual Expenditure: \$544.13K (9/1/2022-8/31/2023)

## **9. Appendices**

Nothing to report.